Energy resolution and non-linearity effects on the neutrino oscillation probability at T2K and beyond

Internship Synopsis
April, 3 – July, 5
2024

Author
Pierre Boistier
M.Sc. student in Physics (M2)
Track NPAC
Faculté des Sciences d'Orsay
Université Paris-Saclay

Supervisor
Dr. Sara Bolognesi
Researcher
Équipe Neutrino accélérateurs
DRF/Irfu/DPhP
CEA Paris-Saclay

Energy resolution and non-linearity effects on the neutrino oscillation probability at T2K and beyond
Internship synopsis. Université Paris-Saclay

© 2024 Pierre Boistier. All rights reserved

This report has been typeset with LaTeX.

Version: April 22, 2024
Author's email: pierre.boistier@universite-paris-saclay.fr

Contents

GENERAL CONTEXT

The concept of the neutrino emerged in the early 20$^{\text{th}}$ century as physicists grappled with the perplexing phenomenon of β decay, in which a radioactive nucleus emits an electron and transforms into a different element. Initially, this process seemed to violate the conservation of energy and momentum, leading Wolfgang PAULI [1] to propose the existence of a new, neutral particle to carry away the missing energy and momentum. In 1930, PAULI postulated the existence of the neutrino ("little neutral one" in Italian), laying the groundwork for decades of experimental exploration. The experimental confirmation of the neutrino came in 1956 through the landmark work of Clyde COWAN and Frederick REINES [2]. Utilizing a neutrino detector at the Savannah River nuclear reactor in the United States, COWAN and REINES successfully observed neutrinos produced in nuclear reactions and detected the telltale signature of neutrino interactions with matter. This historic achievement earned REINES the Nobel Prize in Physics in 1995 and solidified the existence of the neutrino as more than just a theoretical construct. In the 1960s and 1970s, pioneering experiments conducted by Raymond DAVIS Jr. and John BAHCALL [3] uncovered the solar neutrino problem: a discrepancy between the predicted and observed flux of neutrinos from the Sun. DAVIS' Homestake experiment, located deep underground in a South Dakota gold mine, detected a significantly lower number of solar neutrinos than expected based on theoretical Solar models. This puzzling discrepancy sparked decades of research which finally converged into the discovery of the phenomenon known as neutrino oscillations.

Neutrino oscillations, which fundamentally altered our understanding of the Standard Model of particle physics, were first Proposed by Bruno PONTECORVO in the 1950s [4], [5], embedded by Ziro MAKI, Masami NAKAGAWA and Shoichi SAKATA in the 1960s [6], and demonstrated by the Super-Kamiokande (SK) [7] and Sudbury Neutrino Observatory (SNO) [8] experiments in the late 20$^{\text{th}}$, neutrino oscillations imply that neutrinos possess mass and can transform between different leptonic flavour states (electron, muon, and tau) as they propagate through space and time. This discovery shattered the previously held notion that neutrinos were massless and laid the groundwork for a new era of neutrino physics.

Neutrinos also serve as invaluable messengers from the cosmos, providing insights into some of the universe's most extreme environments. High-energy neutrinos produced in astrophysical phenomena such as supernovae, gamma-ray bursts, and active galactic nuclei offer a unique window into the dynamics of these cosmic events. Detectors like IceCube [9], located deep beneath the Antarctic ice, are designed to capture these elusive particles and unravel the mysteries of the high-energy universe.

Neutrinos: the urge to go beyond the Standard Model

Neutrinos are elementary particles of the Standard Model (to go beyond what is exposed hereafter, see *e.g.* [10]). In its current form, they come in three generations and form with the left-handed charged leptons (e_L, μ_L, τ_L) weak isospin doublets. They are of zero mass, zero electric charge, and singlets of the strong interaction. Hence, they can only interact with SM particles through weak interactions, and requires *e.g.* sterile right-handed neutrinos to form a DIRAC mass term through the HIGGS mechanism.

Observations from natural sources – the Sun [8], [11], [12] and cosmic rays interacting with the atmosphere [9], [13], but also from artificial sources – nuclear power plants [14]–[17] and particle accelerators [18]–[20], show a depletion between the expected and the measured neutrino fluxes for specific flavours. This depletion is today well-established to being due to neutrino flavour mixing and oscillation, providing one of the most convincing experimental proofs known today for the existence of physics beyond the Standard Model. Flavour mixing, the same way as for quarks, requires a misalignment between mass eigenstates (ν_1, ν_2, ν_3) and weak flavour eigenstates (ν_e, ν_μ, ν_τ). On the other hand, oscillation requires at least two of the three neutrinos to be massive: measured fluxes only give access to non-vanishing $\Delta m^2_{ij} \equiv {m_i}^2 - {m_j}^2$, leaving the possibility of one massless neutrino among the three generations. This second requirement can be fulfilled by minimally extending the SM with the seesaw mechanisms, adding to the theory, *e.g.* in the case of type-I seesaw, fermionic gauge singlets (right-handed neutrinos).

The canonical way to describe the oscillation and mixing phenomena in the leptonic sector is through the 3×3 PMNS mixing matrix, named for PONTECORVO, MAKI, NAKAGAWA and SAKATA, which describes the neutrino mass eigenstates in terms of the weak flavour eigenstates. In general, there are nine degrees of freedom in any unitary

3×3 matrix. In the case of the PMNS matrix, five of those real parameters can be absorbed as phases of the lepton fields and thus the PMNS matrix can be fully described by four free parameters. The PMNS matrix is most commonly written with the Chau-Keung parametrization as the product of three Tait-Bryan rotations (by θ_{ij}) and a Dirac phase transformation (by δ_{CP}), and reads:

$$U_{\mathrm{PMNS}} = \begin{pmatrix} U_{e1} & U_{e2} & U_{e3} \\ U_{\mu 1} & U_{\mu 2} & U_{\mu 3} \\ U_{\tau 1} & U_{\tau 2} & U_{\tau 3} \end{pmatrix} = \begin{pmatrix} 1 & 0 & 0 \\ 0 & c_{23} & s_{23} \\ 0 & -s_{23} & c_{23} \end{pmatrix} \begin{pmatrix} c_{13} & 0 & s_{13}\,\mathrm{e}^{-i\delta_{\mathrm{CP}}} \\ 0 & 1 & 0 \\ -s_{13}\,\mathrm{e}^{i\delta_{\mathrm{CP}}} & 0 & c_{13} \end{pmatrix} \begin{pmatrix} c_{12} & s_{12} & 0 \\ -s_{12} & c_{12} & 0 \\ 0 & 0 & 1 \end{pmatrix}, \quad (1)$$

where $s_{ij} \equiv \sin\theta_{ij}$ and $c_{ij} \equiv \cos\theta_{ij}$. The angles θ_{ij} can be taken without loss of generality to lie in the first quadrant $[0, \pi/2]$, and the CP phase $\delta_{\mathrm{CP}} \in [0, 2\pi]$. Since a purely real matrix corresponds to δ_{CP} being an integer multiple of π, any other other value is manifested as violation of Charge-Parity symmetry. In the case of Majorana neutrino fields, two extra Majorana complex phases cannot be freely redefined and must be added to the parametrization.

Among these six parameters, θ_{12} and Δm^2_{21} have been measured by solar experiments and KamLAND, a particular reactor neutrino experiment. The parameters θ_{23} (up to an octant degeneracy) and $|\Delta m^2_{32}|$ (only its absolute value) have been measured by atmospheric neutrino experiments. In the last few years, θ_{13} has also been measured by accelerator and reactor experiments. Some aspects are still not constrained: the octant of the mixing angle θ_{23}, the Dirac phase δ_{CP} and the sign of Δm^2_{32}, which can be addressed by improved future measurements at oscillation experiments. Measuring the δ_{CP} phase is crucial as it marks a new fundamental source of CP symmetry violation, the first in the leptonic sector. It is enabled by the different behaviour in flavour oscillations between neutrinos and anti-neutrinos. The sign of Δm^2_{32} is an important issue known as the mass ordering (MO), and is of great interest in the neutrino mass generation mechanism. Its positivity or negativity corresponds, respectively, to the case of normal ($m_2 < m_3$) or inverted ($m_2 > m_3$) mass hierarchy (resp. NO and IO). Some other characteristics remain unknown, such as the Majorana nature of the neutrino, but aren't accessible by oscillation experiments: one must look *e.g.* at processes like the neutrinoless double β decay ($0\nu\beta\beta$), which measurement is strongly correlated with MO [21].

The state of neutrino oscillation research

Neutrino oscillation experiments can be broadly categorized into four main types: solar, atmospheric, accelerator-based, and reactor-based. Solar neutrino experiments are designed to study neutrinos originating from the Sun's core, where nuclear fusion processes produce copious amounts of neutrinos across a broad energy spectrum. These experiments, such as SNO [8] and Borexino [12], provided crucial insights into the processes governing stellar nucleosynthesis and allowed a first look into the neutrino mixing angle θ_{12} and the squared mass difference Δm^2_{21}, later on precisely measured by KamLAND [14], a long-baseline reactor experiment. Atmospheric neutrino experiments investigate neutrinos produced by cosmic ray interactions with the Earth's atmosphere. These experiments, including SK [13] and IceCube [9], observe neutrinos with a wide range of energies and trajectories. By studying the ratio of different neutrino flavours at various energies and zenith angles, atmospheric neutrino experiments can determine neutrino oscillation parameters such as the mixing angle θ_{23}, MO and squared mass difference Δm^2_{32}. They also offer insights into neutrino propagation through different densities of Earth's crust. Reactor-based neutrino experiments utilize the intense flux of antineutrinos emitted during nuclear fission reactions in nuclear power plants. Experiments like Daya Bay [15], Double Chooz [16] and RENO [17] study the disappearance of electron antineutrinos over short baselines, providing precise measurements of the neutrino mixing angle θ_{13} and the composite mass parameter

$$\Delta m^2_{ee} \equiv \Delta m^2_{31} \cos^2\theta_{12} + \Delta m^2_{32} \sin^2\theta_{12}\ . \quad (2)$$

Accelerator-based neutrino experiments utilize high-energy particle accelerators to produce intense beams of neutrinos. These experiments, like the T2K (Tōkai-to-Kamioka) experiment [19] and the NOvA (NuMI Off-Axis ν_e Appearance) experiment [20], generate neutrino beams by accelerating protons and directing them onto target materials, producing a secondary beam of neutrinos through hadron decays (π, κ). Accelerator-based experiments are crucial for studying neutrino oscillations

over long baselines, allowing precise measurements of neutrino mixing parameters such as θ_{23}, Δm^2_{32} and MO. They are of particular importance as they are currently the only oscillation experiments to investigate into CP-violation in the neutrino sector by measuring δ_{CP}.

WORKING ENVIRONMENT

This internship is carried out at Irfu (Institut de recherche sur les lois fondamentales de l'Univers), a CEA (Commissariat à l'Énergie Atomique et aux Énergies Renouvelables) research institute, on the Paris-Saclay site. It is supervised by Dr Sara Bolognesi, researcher in the "Neutrino accélérateurs" team of the DPhP (Département de Physique des Particules).[1] The team has an important history of contributions to the near detector ND280 of the T2K experiment in Japan, and recently started contributing to the HK (Hyper-Kamiokande) experiment. The team is also looking forward contributing to the other future long-baseline experiment, DUNE (Deep Underground Neutrino Experiment), in the USA.

The T2K experiment is conducted in Japan by the international cooperation of about 500 physicists and engineers with over 60 research institutions from several countries from Europe, Asia and North America and is a recognized CERN experiment (RE13). T2K is a long-baseline off-axis neutrino experiment for the study of neutrino oscillations using a beam of muonic neutrinos produced at the J-PARC (Japan Proton Accelerator Research Complex) facility, and measured at short distance (280 m) by the ND280 detectors and at large distance (295 km) by the SK water-Cerenkov detector. T2K collected data within its first phase of operation from 2010 till 2021. The second phase of data taking (T2K-II, with upgraded beam and near detector) will start in 2024 and is expected to last until commencement of the successor of T2K and SK – the HK experiment – in 2027.

The Irfu group has always focused on two complementary aspects of the experiment: detector development and data analysis, specifically of the near detector ND280. It has participated to the design and construction of the set of three large TPCs (Time Projection Chambers) of the near detector ND280 at its creation, and another set of two TPCs during the ND280 Upgrade implementing the resistive Micromegas technology. The group also noticeably contributes in precise measurements of neutrino interaction cross-sections in ND280, by developping tools and models describing such interactions, with the goal of reducing systematic uncertainties in oscillation parameter measurements. Starting in 2020, the group has given a major direct contribution to the oscillation analysis. Firstly, one student performed the fit to the near detector data for the oscillation analysis using the official T2K software. Afterwards, the group proposed an improved fitting framework based on the tools developed in the cross-section measurements. Then from 2022, another student has been the main analyzer for the fit to the far detector data for oscillation analysis. In parallel, the group was engaged in the characterization of the resistive Micromegas detectors deployed in the two new TPCs of the ND280 Upgrade.

The group is today also engaged in the HK project, a megaton-scale water-Cerenkov detector that will give access to the definitive observation of CP-violation in the leptonic sector using neutrinos from J-PARC. It recently started participating in the electronic development at the far detector, and contributing to oscillation sensitivity studies.

I. LONG-BASELINE ACCELERATOR OSCILLATION EXPERIMENTS

Long-baseline neutrino experiments play a pivotal role in elucidating the intricacies of neutrino oscillations, enhanced by recent years of remarkable advancements in accelerator and detector technology. The accelerators produce intense beams of high-energy protons, which are directed onto a target material to generate a secondary beam of mesons, primarily pions and kaons. The secondary mesons decay into neutrinos and other particles, predominantly muons. The resulting neutrinos, which come in different leptonic flavours, are directed towards a distant detector site. We therefore define the experiment baseline as the distance between the source target and the far detector. To maximize the probability of detecting neutrino oscillations, the neutrino beam is typically tuned to a specific energy range corresponding, given the baseline, to the neutrino oscillation maximum. In long-baseline neutrino experiments, the principle of having both a near detector (ND) and a far detector (FD) is fundamental to precisely study neutrino oscillations. The ND is positioned relatively close to the neutrino source, typically

1. The complete name of the lab being CEA/Paris-Saclay/DRF/Irfu/DPhP, DRF standing for "Direction de la recherche fondamentale".

within a few hundred meters. Its primary purpose is to characterize the initial properties of the neutrino beam shortly after its production. Since the neutrinos have just been generated and haven't traveled a significant distance, the ND measures the neutrinos before oscillation, providing a baseline reference for comparison. The FD is located at a considerable distance from the neutrino source, often hundreds to thousands of kilometers away. Its primary function is to detect neutrinos after they have traveled enough to oscillate. The FD is equipped with sensitive detection systems capable of capturing neutrino interactions and identifying the flavour of the outgoing particles. Comparing the neutrino properties observed at the FD to those measured at the ND enables scientists to infer the parameters governing neutrino oscillations, such as the mixing angles and mass differences between different neutrino flavours. The combination of near and far detectors provides a powerful means of disentangling the effects of neutrino oscillations from other factors, such as beam uncertainties, neutrino-nucleus interactions and detector effects. These detectors are typically located deep underground to shield them from cosmic rays. Different detection techniques, such as scintillation, CERENKOV radiation, or liquid Argon TPC, are employed to identify and characterize neutrino interactions.

Among long-baseline neutrino accelerator experiments, the NOvA experiment and T2K experiment have significantly advanced our understanding of neutrino oscillations. T2K, located in Japan, utilizes a beam produced at J-PARC in Tōkai. This beam consists primarily of muon neutrinos, directed towards the SK detector, situated 295 km away in Kamioka. Operating with a similar principle to T2K, NOvA utilizes the NuMI (Neutrinos at the Main Injector) beam, at Fermilab near Chicago, Illinois, USA. This beam travels across 810 km to the NOvA FD located in northern Minnesota. Looking ahead, the HK experiment, set to be located in Japan and take over T2K and SK, and the DUNE experiment, set to be constructed at the Sanford Underground Research Facility in the USA, will leverage cutting-edge detector technologies and powerful neutrino beams to probe neutrino oscillation properties with unprecedented precision.

II. THE T2K EXPERIMENT

The T2K experiment [19], [25] is a second-generation accelerator neutrino oscillation experiment in Japan, which operates a narrow-band beam along a 295 km baseline, stretching from the J-PARC facility in Tōkai, Ibaraki, to the SK detector in Hida, Gifu. The primary proton beam is accelerated to 30 GeV at J-PARC's Main Ring. These protons are delivered in eight bunches per cycle, before impinging on a 91.4 cm graphite target to produce a secondary beam, predominantly yielding pions and kaons. The particles are then focused using magnetic horns, which currents determine which charge is focused and defocused, and navigates a 96 m Helium-filled decay volume where they can decay into neutrinos (or antineutrinos, depending on the horns' polarity) and other particles. A beam dump sits at the end of the decay volume, followed by a muon monitor (MUMON). Employing the off-axis method, the outgoing neutrino beam is directed at a 2.5° angle with respect to the baseline connecting the proton target and the FD, which enhances the flux at the peak energy (600 MeV) while reducing the higher energy component that produces background events and improving the ν_μ/ν_e ratio.

The orientation of the magnetic horns determines the nature of the neutrino beam. In the 'Forward Horn Current' (FHC) mode, positively-charged secondaries yield a predominantly ν_μ beam, while the 'Reversed Horn Current' (RHC) mode generates a beam primarily composed of $\overline{\nu}_\mu$. Both configurations entail a fraction of 'wrong-sign' flux, necessitating meticulous background subtraction methodologies.

The experiment incorporates a suite of ND located approximately 280 m downstream of the target. The INGRID detector, stationed on the nominal beam axis, provides real-time monitoring of neutrino beam intensity and direction. Meanwhile, the ND280 off-axis detector, optimized for characterizing neutrino interactions, furnishes crucial data for constraining flux uncertainties and discerning neutrino properties. Until 2023, the ND280 detector was composed of: a water-scintillator detector optimized to identify π^0 (the P0D); the tracker consisting of time projection chambers (TPCs) and fine grained detectors (FGDs) optimized to study charged current interactions; and an electromagnetic calorimeter (ECal) that surrounds the P0D and the tracker. The whole detector is placed in a 0.2 T magnetic field provided by the recycled UA1 magnet, which also serves as part of a side muon range detector (SMRD).

ND280 is currently undergoing an update before the experiment's second run, T2K-II. The aim is to improve the performance by adding a new highly granular, 3D scintillator detector, Super-FGD composed of small plastic scintilla-

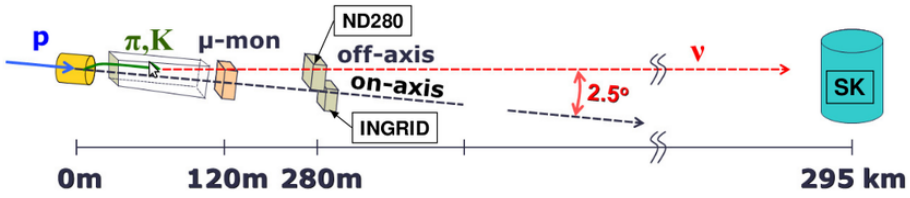

Figure 1 *– Overview of the T2K experiment from the proton beamline (blue) at J-PARC, to the neutrino beam (red), with schematic of the target, the decay volume, the MUMON, the near detectors (INGRID, ND280) and the far detector (SK). Extracted from [22].*

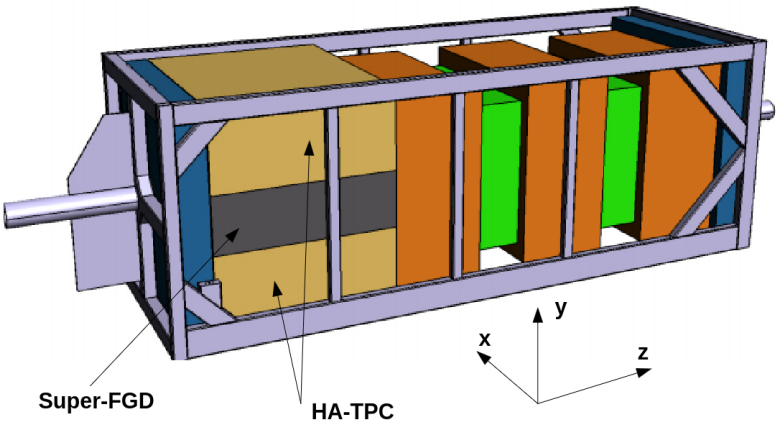

Figure 2 *– CAD 3D Model of the ND280 upgrade detector. In the upstream part (on the left in the drawing) two High-Angle TPCs (brown) with the scintillator detector Super-FGD (gray) in the middle will be installed. In the downstream part, the tracker system composed by three TPCs (orange) and the two FGDs (green) will remain unchanged. The time-of-flight detectors are not shown in this plot. Extracted from [23].*

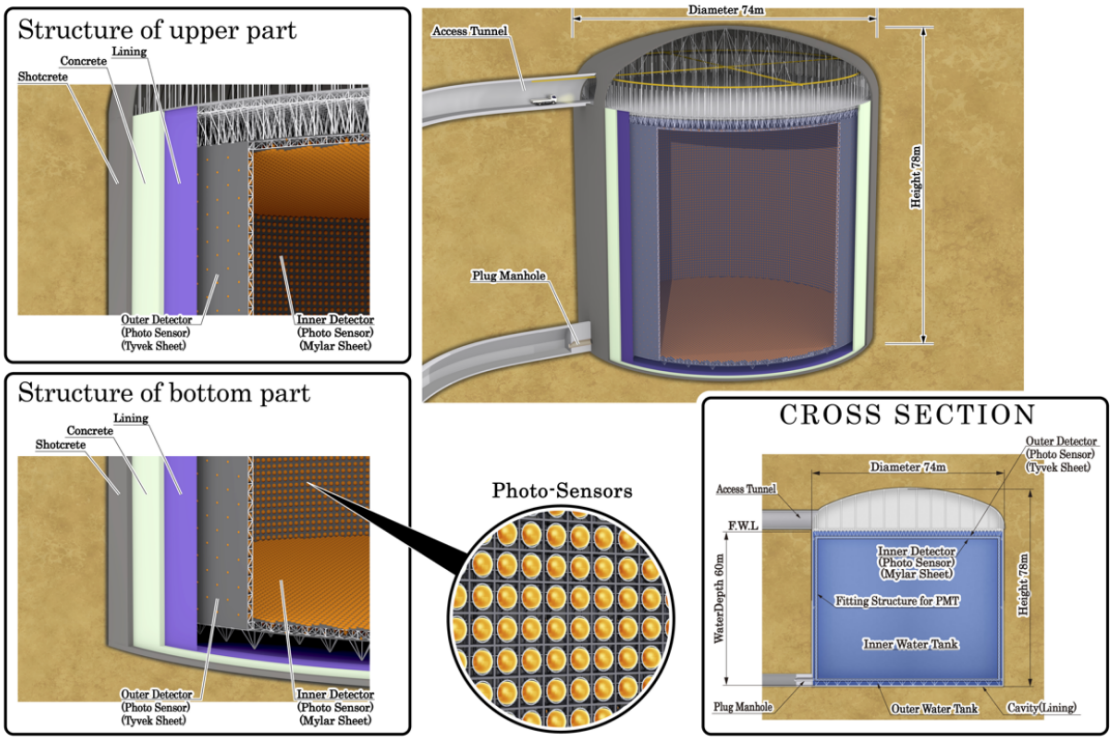

Figure 3 *– Schematic view for the configuration of HK far detector: a single cylindrical tank instrumented with high density (40% photocoverage) PMTs. Extracted from [24].*

tor cubes, read out by three Wavelength Shifting (WLS) fibers in the three orthogonal directions. Above and below this detector are two High-Angle atmospheric pressure TPCs, implementing the resistive Micromegas technology. While the present configuration of ND280 leads to systematic errors of the order of 6%, the goal is to bring this number down to $\sim 4\%$ for T2K-II, and to $\sim 3\%$ or below for HK. [23]

Situated 4 km south and 12 km below the beam axis, the SK detector is composed of a vertical water tank holding 50 kt of ultra-pure water, separated into an inner detector (ID) and an outer detector (OD). The OD serves as a veto detector for cosmic rays and a shield against external backgrounds. A stainless steel supporting structure separates the ID and OD, housing 13 014 PMTs in total. Events are categorized based on the Cerenkov light patterns, distinguishing between muon- and electron-like signatures. The absence of a magnetic field implies the utilization of the horn current polarity as a proxy for neutrino/antineutrino discrimination.

In the meanwhile, the HK collaboration is preparing the next-generation water-Cerenkov detector that will benefit from the J-PARC facility as shown in Fig. 3. HK's fiducial volume will be 8 times larger (258 kt of water) than the SK detector and a beam 3 times more powerful than the one currently used at T2K. The design will be similar to SK's, divided into an ID and an OD, and will hold more than 20 000 PMTs. Located 8 km south from the SK detector, it will be at the same off-axis angle and at the same distance from J-PARC. The expected precision of HK is a 5σ significance CP violation discovery, a 5σ MO determination with atmospheric neutrinos and precision measurements of Δm^2_{32} and $\sin^2\theta_{23}$ at less than 2%. In order to reach such targets, the energy scale uncertainty for HK should be about 0.5%, whereas the current error at SK is of 2%. [26]

III. THE INTERNSHIP PROJECT

Goals and timeline

The aim of the internship is to study the effects of the neutrino energy resolution and energy scale bias, at T2K and further beyond at HK, in order to see how it affects the experiment's sensitivity to the parameters of the oscillation probability. The starting point will be the study of a `Python3` code written by a Ph.D. student of the team, Denis Carabadjac. The code implements the flavour oscillation formula, given the beam and baseline parameters. Then, the code will be enhanced by convoluting the oscillation formula with the flux of produced neutrinos and their interaction cross-section, complying with the T2K and the future HK configurations. The simulation will be very basic but its flexibility will allow a first-order wide-ranging study. Finally, the code will be used to study the effects of the energy resolution and non-linearity bias on the oscillation parameters. This study will be focused on T2K and HK, but could also be applied on DUNE-like configuration, in order to study different resolutions and flux energies.

The internship lasts 13 weeks, from April, 3rd until July, 5th. The proposed timeline is the following:

- bibliography, study of the `Python3` code by Denis Carabadjac, writing the synopsis (*2-4 weeks*);
- implementing the convolution of the oscillation with the flux of produced neutrinos and their interaction cross-section (*4 weeks*);
- applying the code to the study of the energy resolution and bias effects on the oscillation parameters (*4 weeks*).

One extra week is preserved for both the preparation to the Doctoral School examination (end of May) and NPAC oral examination (end of June). Naturally, the internship work will be sprinkled by lab life, such as team meetings, conferences, workshops, etc.

The main advisors to the project will be the internship supervisor, Sara Bolognesi, and the code's first contributor, Denis Carabadjac.

Neutrino oscillation

Starting from the PMNS matrix (1), assuming three neutrino generations, we denote mass eigenstates by $|\nu_i\rangle$, $i \in \{1,2,3\}$ and weak flavour eigenstates by $|\nu_\alpha\rangle$, $\alpha \in \{e,\mu,\tau\}$, so that one can connect them writing

$$|\nu_\alpha\rangle = \sum_i U^*_{\alpha i} |\nu_i\rangle \ . \tag{3}$$

A given neutrino is produced as a pure weak flavour eigenstate, propagates as a linear combination of interfering mass eigenstates, and is detected or interacts as weak pure flavour eigenstate. Then, one must look at oscillation probability from some flavour state α to some flavour state β. We particularly speak of the appearance probability of β, if $\beta \neq \alpha$, and the disappearance probability of α if $\alpha = \beta$. Hence, the vacuum oscillation probability

$\mathcal{P}_{\alpha\to\beta}$ for a state ν_α to oscillate into ν_β after some time t is given by

$$\mathcal{P}_{\alpha\to\beta}(t) = \left| \sum_i \sum_j U^*_{\alpha i} U_{\beta j} \langle \nu_j | \nu_i(t) \rangle \right|^2 . \quad (4)$$

Since $|\nu_j\rangle$ are mass eigenstates, their propagation through space and time follow the SCHRÖDINGER equation and can be approximated as plane wave solutions, here and hereafter using natural units:

$$|\nu_j(t)\rangle = \exp\left(-i\left(E_j t - \mathbf{p}_j \cdot \mathbf{x}\right)\right) |\nu_j(0)\rangle \ , \quad (5)$$

where E_j, $\mathbf{p}_j$, $\mathbf{x}$ are respectively the energy, momentum, position of the $|\nu_j\rangle$ state. The plane wave description is a rather rough approximation, but a similar computation using wavepackets description leads to the same oscillation probability [10].

In the ultra-relativistic limit (always satisfied for current oscillation experiments, since the neutrinos have mass $m \lesssim \mathcal{O}(1\text{ eV})$ and energy $E \gtrsim \mathcal{O}(1\text{ MeV})$ [25]), we have $p_j \gg m_j$. Hence the mass eigenstate energy reads

$$E_j = \sqrt{{p_j}^2 + {m_j}^2} \simeq p_j + \frac{{m_j}^2}{2\,p_j} \simeq E + \frac{{m_j}^2}{2\,E} \ , \quad (6)$$

where E is the total energy of the particle. Using also $t \simeq L$ where L is the distance traveled by neutrinos (the baseline of the experiment), and dropping the global phase factors that will not contribute to the probability, we can rewrite (5) as

$$|\nu_i(L)\rangle = \exp\left(-i\left(\frac{{m_j}^2 L}{2\,E}\right)\right) |\nu_j(0)\rangle \ . \quad (7)$$

Finally, taking (4) and (7), and noting the orthogonality of the eigenstates $\langle \nu_i | \nu_j \rangle = \delta_{ij}$, we can conclude after some computations by expanding the vacuum oscillation probability as

$$\begin{aligned} \mathcal{P}_{\alpha\to\beta}(E,L) = \delta_{\alpha\beta} &- 4 \sum_{i>j} \mathrm{Re}(U^*_{\alpha i} U_{\alpha j} U_{\beta i} U^*_{\beta j}) \sin^2 X_{ij} \\ &\pm 2 \sum_{i>j} \mathrm{Im}(U^*_{\alpha i} U_{\alpha j} U_{\beta i} U^*_{\beta j}) \sin\left(2X_{ij}\right) \ , \end{aligned} \quad (8)$$

where we use above and hereafter $X_{ij} \equiv \Delta m^2_{ij} L/4E$ and where the + (resp. −) sign stands for neutrino (resp. antineutrino) states. Consequently, we conclude that the second term on the right hand-side in (8) is CP conserving since it is the same for neutrinos and anti-neutrinos, whilst the last one is CP violating due to the sign difference. One can hence define the CP asymmetry Δ_{CP} as

$$\begin{aligned} \Delta_{\mathrm{CP}}(\alpha\beta) &\equiv \mathcal{P}^{\nu}_{\alpha\to\beta} - \mathcal{P}^{\overline{\nu}}_{\alpha\to\beta} \\ &= 4 \sum_{i>j} \mathrm{Im}(U^*_{\alpha i} U_{\alpha j} U_{\beta i} U^*_{\beta j}) \sin(2X_{ij}) \ . \end{aligned} \quad (9)$$

Thanks to the CPT theorem, one can express (9) as follows

$$\begin{aligned} \Delta_{\mathrm{CP}} &\equiv \Delta_{\mathrm{CP}}(e\mu) = \Delta_{\mathrm{CP}}(\mu\tau) = \Delta_{\mathrm{CP}}(\tau e) \\ &= 16 \mathcal{J} \sin(2X_{12}) \sin(2X_{23}) \sin(2X_{31}) \ , \end{aligned} \quad (10)$$

where $\mathcal{J}$ is the JARLSKOG invariant,

$$\mathcal{J} \equiv \mathrm{Im}(U^*_{e1} U_{e3} U_{\mu 1} U^*_{\mu 3}) \ , \quad (11)$$

which is directly proportional to $\sin\delta_{\mathrm{CP}}$.

In the T2K configuration (but also in every long-baseline neutrino experiments), the neutrino beam has to travel the Earth's crust before encountering the FD. In that way, neutrinos can interact with matter, predominantly via weak Charged Current (CC) interactions with electrons (Neutral Current (NC) interactions don't contribute to the total probability since they are identical regardless of the flavour). Hence, the propagation Hamiltonian used to obtain the plane wave solutions (5) has to be adjusted by a potential

$$V = \pm\,\mathrm{diag}(1,0,0)\sqrt{2}\,G_F\,n_e \ , \quad (12)$$

where n_e is the number density of electrons, G_F is the FERMI coupling constant, and the − sign applies for antineutrinos. The other terms of the diagonal read zero since there aren't any μ's or τ's in the crust for neutrinos to interact with. Here we assumed the density of electrons to be constant along the baseline, which is a good approximation for long-baseline accelerator experiments. The matter effect potential (12) has non-negligible implications on the CP asymmetry (9).

Simplified oscillation probability at T2K

In the case of T2K, it is possible to make some reasonable and useful approximations for a qualitative understanding of the oscillation effect. At first order, one can approximate the matter effects of the oscillation probability to zero, since taking the

current values from the NuFit collaboration in appendix Fig. 11 and a crust density of 2.6 $\mathrm{cm}\cdot\mathrm{g}^{-1}$ [27] leads to

$$\underset{250}{\Delta m^2_{31}} \gg 2\sqrt{2}G_F n_e E \gtrsim \underset{7.4}{\Delta m^2_{21}}\,. \quad \underset{11.9}{} \quad (\times 10^{-5}\ \mathrm{eV}^2) \tag{13}$$

The baseline from J-PARC to SK is approximately $L \simeq 295$ km and the mean energy of the muon neutrino beam is $E \simeq 0.6$ GeV. Hence, we can estimate the $\sin^2 X_{21}$ terms to be negligible compared to the $\sin^2 X_{31}$ terms which realizes a maximum of the oscillation. Note that T2K parameters have been chosen so that the oscillation probability of the ν_μ beam is at a resonance at SK. At first order, the oscillation probability of the ν_e appearance channel and the ν_μ disappearance channel read

$$\mathcal{P}^{\nu}_{\mu\to e} \simeq \sin^2(2\,\theta_{13})\sin^2\theta_{23}\sin^2\left(X_{31}\right)\ , \tag{14}$$

$$\mathcal{P}^{\nu}_{\mu\to\mu} \simeq 1-\sin^2(2\,\theta_{23})\cos^4\theta_{13}\sin^2\left(X_{32}\right)\ . \tag{15}$$

The un-approximated formula for the ν_e appearance channel can be seen as an example in the appendix at equation (21), where one can notably see the matter effects taken into account. Looking at the ν_μ disappearance channel and using Carabadjac's `Python3` simulation, one can see in Fig. 4 that amplitude and frequency of the oscillation are directly linked to $\sin^2(2\,\theta_{23})$ and Δm^2_{32} respectively. However, the factor 2 in the sine implies a degeneracy of the θ_{23} measurement, the so-called octant degeneracy: the angle can be measured in this channel modulo $\pi/4$. Hence, a second measurement is required, and can be achieved looking at the ν_e appearance channel shown in Fig. 5. This channel is dominated by θ_{13}, but that parameter is well measured by reactor experiments. Therefore, exploiting θ_{13} measurements from those reactor experiments, the ν_e appearance channel can be used to break the θ_{23} degeneracy, as shown in Fig. 6.

In order to measure δ_{CP} and MO, one can look at the CP asymmetry (9) and approximate the Jarlskog invariant to leading order

$$\mathcal{J} \simeq \sin(2\,\theta_{23})\sin(2\,\theta_{12})\sin\theta_{13}\sin\delta_{\mathrm{CP}}\ . \tag{16}$$

Hence, the CP asymmetry is governed by several parameters: we know θ_{23}, θ_{12}, Δm^2_{31}, Δm^2_{21} to be large, and more recently θ_{13} to be non-zero but small. The only remaining parameter to measure in order to observe CP violation, *i.e.* $\Delta_{\mathrm{CP}} \neq 0$, is the CP phase δ_{CP} which must be non zero. More convenient in the oscillation analysis is to define

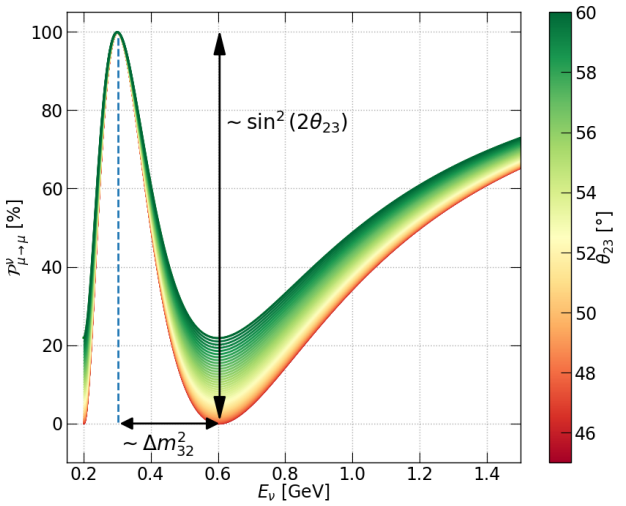

Figure 4 – *Oscillation probability as a function of the energy in the ν_μ disappearance channel with T2K parameters. Plot from Carabadjac.*

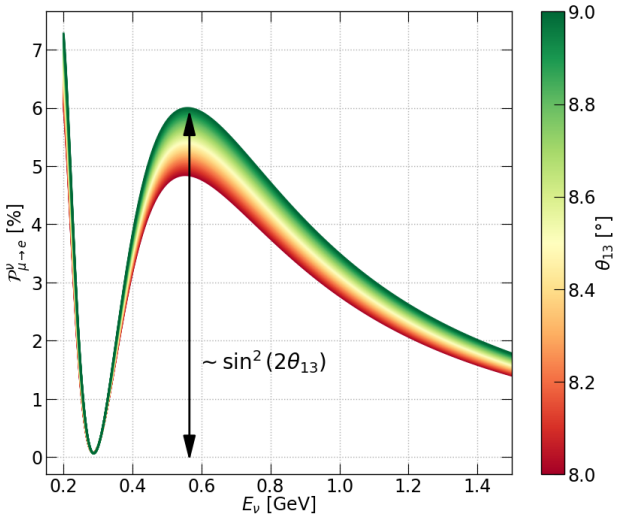

Figure 5 – *Oscillation probability as a function of the energy in the ν_e appearance channel with T2K parameters. Plot from Carabadjac.*

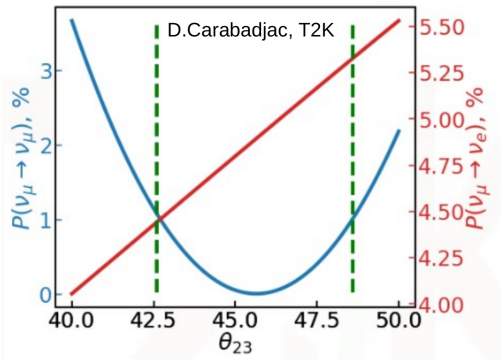

Figure 6 – *Oscillation probability as a function of the mixing angle θ_{23} in the ν_e appearance channel (red) and in the ν_μ disappearance channel (blue) with T2K parameters. Plot from Carabadjac.*

the relative CP asymmetry $\mathcal{A}_{\text{CP}}$ as

$$\mathcal{A}_{\text{CP}} \equiv \frac{\mathcal{P}^{\nu}_{\mu\to e} - \mathcal{P}^{\overline{\nu}}_{\mu\to e}}{\mathcal{P}^{\nu}_{\mu\to e} + \mathcal{P}^{\overline{\nu}}_{\mu\to e}} \ . \tag{17}$$

As above, we can approximate it as

$$\mathcal{A}_{\text{CP}} \simeq -\frac{\sin(2\theta_{12})\sin\delta_{\text{CP}}}{\sin\theta_{13}\tan\theta_{23}} + \text{matter} \ , \tag{18}$$

where we ignore hereafter the matter effects for the sake of simplicity. Hence plotting (18) as a function of δ_{CP} in Fig. 7, one can see that the CP phase has up to a 30% effect if maximal CP-violation, while MO has a 10% effect. These measurements are once again accessible only if the other oscillation parameters in (16) are known up to the percent, especially θ_{13}. Collaboration with other types of oscillation experiments is thus crucial.

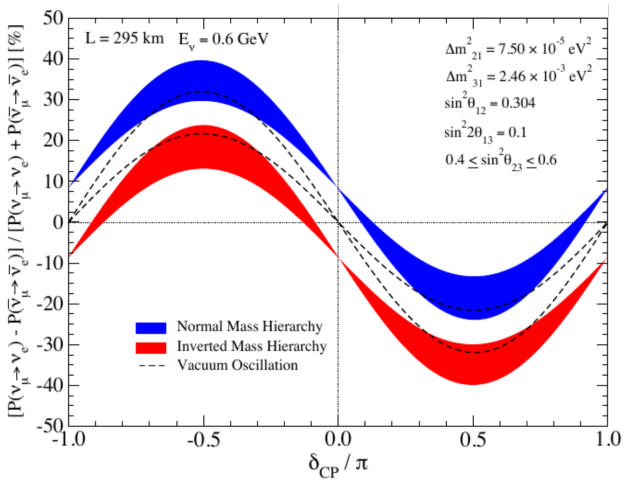

Figure 7 *– Relative CP asymmetry as a function of normalized δ_{CP} with T2K parameters. Matter effects are neglected. Extracted from [24].*

The experimental framework

The aim of long-baseline neutrino experiments is to measure the different parameters accessible through neutrino oscillations: PMNS angles θ_{ij}, the CP phase δ_{CP}, masses squared Δm^2_{ij} and MO. As seen previously, those parameters are accessible through the oscillation probability, via appearance and disappearance channels. Hence, the probability has to be computed by modeling and tuning the fluxes of neutrinos at the target source and their interaction cross-sections with matter. For instance, we can express the numbers N_β of neutrinos ν_β at the FD as

$$N_\beta\left(\overline{E}\right) \simeq \int \mathrm{d}E \ \left[\mathcal{P}_{\alpha\to\beta}(E,L) \times \Phi_\alpha(E) \times \sigma_\beta(E) \times \varepsilon_{\text{det}} \times d\left(E,\overline{E}\right)\right] \ , \tag{19}$$

with $\overline{E}$ the reconstructed energy; Φ_α the flux of α neutrinos produced at the accelerator facility; σ_β the neutrino interaction cross-section with matter; ε_{det} the detector efficiency; $d(E,\overline{E})$ the migration matrix between the true neutrino energy E and the reconstructed neutrino energy $\overline{E}$. Here, the dependence on the energy is crucial and due to the fact that the neutrino beam is not monochromatic. The number of detected neutrinos, their reconstructed energy and their flavour are the accessible input, whereas the oscillation probability $\mathcal{P}_{\alpha\to\beta}$ is the unknown we want to estimate. This necessitates the consideration of three distinct categories of systematic uncertainties: those associated with the flux, with the interaction cross-section, and with the detector. Moreover, a thorough understanding of background processes and a mapping between true energy and observable quantities, is crucial for accurately reconstructing the oscillation probability. The ND is used to tune the model, which is then extrapolated to the FD. However, this tuning is of particular complexity since the only accessible observables are outgoing particles from neutrino interactions. Moreover, the flux and the interaction cross-section are highly anti-correlated, so that other experiments are required to help disentangle their effects before extrapolation, such as NA61 at CERN, which is used to tune the flux.

The neutrino energy reconstruction

To the considered energies at T2K (the neutrino energy $E \in \mathcal{O}([100\ \text{MeV}, 1\ \text{GeV}])$), several nuclear interaction processes may occur, as one can see in Appendix Fig. 12, and one of which is dominant: the charged-current quasi-elastic (CCQE) interaction, where the neutrino transforms into the associated lepton, exchanging a W with a nucleon, as illustrated in Fig. 8.

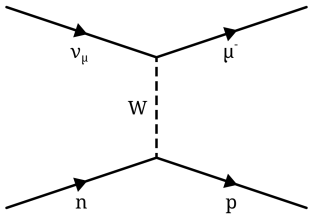

Figure 8 *– FEYNMAN diagram of a ν_μ CCQE interaction.*

For CCQE interactions, neutrino energy can be reconstructed using final-state charged-lepton

kinematics only

$$E_{\mathrm{QE}}^{\mathrm{Rec}} = \frac{2M_{N,i}E_\ell - {M_\ell}^2 + {M_{N,f}}^2 - {M_{N,i}}^2}{2(M_{N,i} - E_\ell + p_\ell \cos\theta_\ell)} \ , \quad (20)$$

where $M_{N,i}$, $M_{N,f}$ and M_ℓ are the mass of the initial-state nucleon (an effective, off-shell mass that includes the nucleon removal energy), final-state nucleon and final-state charged lepton respectively; E_ℓ, p_ℓ and θ_ℓ are the energy, momentum and angle of the final-state charged-lepton respectively. In the current T2K analysis, neutrino energy reconstruction relies solely on lepton kinematics, both at the ND and FD. Nonetheless, this approach faces limitations due to nuclear effects in neutrino interactions. It fails to account for instances where interactions might be misidentified as CCQE due to nuclear effects, such as neutrino scattering off a bound state of two nucleons (referred to as 2p2h reaction) or charged-current reactions resulting in non-reconstructed or absorbed pions (known as final state interactions, FSI, for pions).

Furthermore, nuclear effects like Fermi motion and removal energy add complexity. Fermi motion causes a broadening of the neutrino energy reconstruction, while removal energy introduces a bias in the reconstructed energy. These next-order effects are noticeably visible when plotting an energy reconstruction model in Fig. 9. Many systematic uncertainties in energy reconstruction directly affect the measurement of neutrino oscillation parameters.

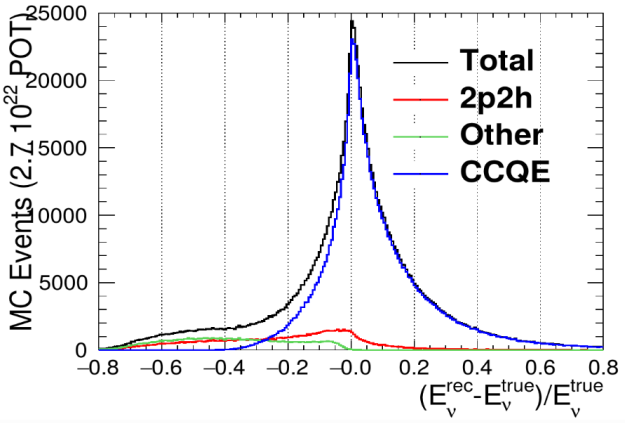

Figure 9 *– Normalized difference between neutrino reconstructed and true energies. The model takes into account CCQE (blue), 2p2h (red) and other (green, amounts for CC where the pion is absorbed in nucleus by FSI). Extracted from a T2K internal communication.*

At T2K's far detector, SK, neutrinos are detected when they interact with the water and produce charged particles above the Cerenkov threshold, and the cone of light emitted by a charged particle is observed as a ring by the PMTs on the detector wall. For each event the time of the first photon arrival as well as the integrated charge at each PMT is recorded, and from that information the type and the kinematics of the particles are inferred and used to reconstruct the energy using (20). The reconstruction process for events within the SK detector unfolds in four sequential stages. Initially, an event vertex is pinpointed based on the timing of the PMT hits, while the direction of the initial track is deduced by identifying a distinct edge in the PMT charge distribution. Subsequently, an iterative algorithm employs a Hough transform of the PMT charge distribution to identify potential Cerenkov ring formations. In the third stage, a particle identification (PID) algorithm categorizes all detected ring candidates as either muon-like or electron-like, achieved by comparing the observed charge pattern with an analytically derived pattern for muons and a simulated pattern for electrons. Finally, the momentum of each particle is reconstructed by analyzing the distribution of observed charge associated with its Cerenkov ring. This correlation between observed charge and particle momentum is established through Monte Carlo simulations and detector calibration, making use of multiple sources (laser light, radioactive sources and a LINAC) as well as dedicated control samples (stopping muons, π^0 events). Hence, on top of energy smearing due to nuclear effects, additional detector effects must be considered in the measurement of the lepton momentum and angle. A fine knowledge of the energy resolution and bias induced by the FD calibration is critical. In Fig. 10, we present an event display featuring two T2K neutrino beam interaction events. The left panel exhibits a Cerenkov ring characterized as muon-like, displaying a distinct outer ring edge, contrasting with the electron-like Cerenkov ring depicted in the right panel, notable for its blurred edges.

As models exist for fluxes, interaction cross-sections and energy reconstruction, systematic studies of the two firsts' dependency on the oscillation parameters precision has been conducted at T2K, but not specifically and separately for the last one. This internship takes place in this context and aim at studying the effects of the energy model on the oscillation measurement. Such study will allow to quantify the requirements needed at the ND to constrain the reconstructed energy model and the requirements on the energy resolution and bias at the FD for precision measurements.

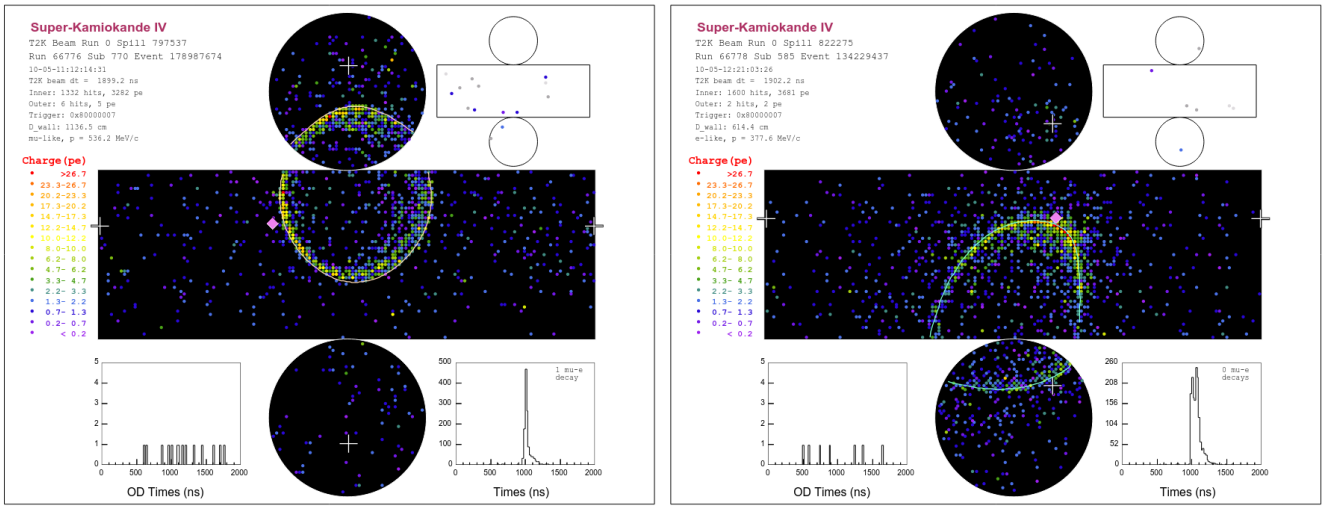

(a) muon-like event

(b) electron-like event

Figure 10 – *Example of reconstructed T2K events in SK for (a) a muon-like ring and (b) an electron-like ring. Both figures show the cylindrical detector, unrolled onto a plane. Each colored point represents a PMT, with the color corresponding to the amount of charge, and the reconstructed cone is shown as a white line. The second figure in the upper right corner shows the same hit map for the OD. The white crosses indicate the location of the reconstructed vertex. The diamond marks the location where a ray starting from the event vertex and heading in the direction of the beam would intersect the detector wall. Extracted from [19].*

CONCLUSION AND OUTLOOK

The neutrino field has witnessed significant advancements, reshaping our understanding of the universe. In the near future, it is poised to reveal critical insights into phenomena such as leptonic CP-violation and the neutrino mass hierarchy. T2K, as one of the present two leading long-baseline accelerator experiments, has made notable progress in precision measurements of oscillation parameters. With its upcoming run, T2K aims to enhance its sensitivity to δ_{CP}, $|\Delta m^2_{32}|$ and θ_{23}. The T2K group at CEA is a key contributor to these advancements.

Systematic uncertainties from energy reconstruction, particularly nuclear effects and detector performances, remain significant challenges, even more as entering the era of precision oscillation measurements. These uncertainties hinder current oscillation measurements in T2K and are expected to become dominant in future experiments like DUNE and HK. Addressing these uncertainties is crucial for advancing neutrino physics.

The forthcoming exploration of energy resolution and non-linearity effects on neutrino oscillation probability promises to be enlightening in various aspects: particularly in the evaluation of systematic uncertainties at T2K and in the design of HK detector calibration system. Moreover, the findings are anticipated to facilitate meaningful comparisons with energy resolution in other experiments, such as DUNE.

This internship serves as a vital component of my scientific trajectory, laying the groundwork for my forthcoming thesis. The hands-on experience gained in neutrino oscillation analysis will significantly bolster my understanding of experimental techniques, data interpretation, and statistical methods essential for conducting rigorous research in this field. This acquired expertise will be instrumental in shaping the trajectory of my thesis, which aims to delve deeper into the intricacies of long-baseline accelerator neutrino oscillation experiments.

References

[1] W. Pauli, « Letter addressed to the participants of the Tübingen conference on radioactivity », *Pauli Letter Collection, CERN archives*, 1930. [Online]. Available: https://cds.cern.ch/record/83282.

[2] C. L. Cowan, F. Reines, F. B. Harrison, H. W. Kruse, and A. D. McGuire, « Detection of the free neutrino: a confirmation », *Science*, vol. 124, no. 3212, pp. 103–104, 1956. DOI: 10.1126/science.124.3212.103.

[3] J. N. Bahcall and R. Davis, « Solar neutrinos: a scientific puzzle », *Science*, vol. 191, no. 4224, pp. 264–267, 1976. DOI: 10.1126/science.191.4224.264.

[4] B. Pontecorvo, « Mesonium and anti-mesonium », *Sov. Phys. JETP*, vol. 6, p. 429, 1957.

[5] B. Pontecorvo, « Inverse beta processes and nonconservation of lepton charge », *Zh. Eksp. Teor. Fiz.*, vol. 34, p. 247, 1957.

[6] Z. Maki, M. Nakagawa, and S. Sakata, « Remarks on the unified model of elementary particles », *Prog. Theor. Phys.*, vol. 28, pp. 870–880, 1962. DOI: 10.1143/PTP.28.870.

[7] Y. Fukuda, T. Hayakawa, E. Ichihara, *et al.*, « Evidence for oscillation of atmospheric neutrinos », *Physical Review Letters*, vol. 81, no. 8, pp. 1562–1567, Aug. 1998, ISSN: 1079-7114. DOI: 10.1103/physrevlett.81.1562.

[8] Q. R. Ahmad, R. C. Allen, T. C. Andersen, *et al.*, « Measurement of the rate of $\nu_e + d \rightarrow p + p + e^-$ Interactions Produced by ^8B solar neutrinos at the Sudbury Neutrino Observatory », *Physical Review Letters*, vol. 87, no. 7, Jul. 2001, ISSN: 1079-7114. DOI: 10.1103/physrevlett.87.071301.

[9] M. G. Aartsen, M. Ackermann, J. Adams, *et al.*, « Measurement of atmospheric neutrino oscillations at 6–56 GeV with IceCube DeepCore », *Phys. Rev. Lett.*, vol. 120, p. 071 801, 7 Feb. 2018. DOI: 10.1103/PhysRevLett.120.071801.

[10] C. Giunti and C. W. Kim, *Fundamentals of Neutrino Physics and Astrophysics*. Oxford University Press, 2007.

[11] K. Abe, Y. Haga, Y. Hayato, *et al.*, « Solar neutrino measurements in Super-Kamiokande-IV », *Phys. Rev. D*, vol. 94, p. 052 010, 5 Sep. 2016. DOI: 10.1103/PhysRevD.94.052010.

[12] S. Kumaran, L. Ludhova, Ö. Penek, and G. Settanta, « Borexino results on neutrinos from the Sun and Earth », *Universe*, vol. 7, no. 7, p. 231, Jul. 2021, ISSN: 2218-1997. DOI: 10.3390/universe7070231.

[13] K. Abe, C. Bronner, Y. Haga, *et al.*, « Atmospheric neutrino oscillation analysis with external constraints in Super-Kamiokande I-IV », *Phys. Rev. D*, vol. 97, p. 072 001, 7 Apr. 2018. DOI: 10.1103/PhysRevD.97.072001.

[14] A. Gando, Y. Gando, H. Hanakago, *et al.*, « Reactor on-off antineutrino measurement with KamLAND », *Phys. Rev. D*, vol. 88, p. 033 001, 3 Aug. 2013. DOI: 10.1103/PhysRevD.88.033001.

[15] D. Adey, F. P. An, A. B. Balantekin, *et al.*, « Measurement of the electron antineutrino oscillation with 1958 days of operation at Daya Bay », *Phys. Rev. Lett.*, vol. 121, p. 241 805, 24 Dec. 2018. DOI: 10.1103/PhysRevLett.121.241805.

[16] Y. Abe, S. Appel, T. Abrahão, *et al.*, « Measurement of θ_{13} in Double Chooz using neutron captures on hydrogen with novel background rejection techniques », *Journal of High Energy Physics*, vol. 2016, no. 1, Jan. 2016, ISSN: 1029-8479. DOI: 10.1007/jhep01(2016)163.

[17] G. Bak, J. H. Choi, H. I. Jang, *et al.*, « Measurement of reactor antineutrino oscillation amplitude and frequency at RENO », *Phys. Rev. Lett.*, vol. 121, p. 201 801, 20 Nov. 2018. DOI: 10.1103/PhysRevLett.121.201801.

[18] M. H. Ahn, E. Aliu, S. Andringa, *et al.*, « Measurement of neutrino oscillation by the K2K experiment », *Phys. Rev. D*, vol. 74, p. 072 003, 7 Oct. 2006. DOI: 10.1103/PhysRevD.74.072003.

[19] K. Abe, N. Abgrall, H. Aihara, *et al.*, « The T2K experiment », *Nuclear Instruments and Methods in Physics Research Section A*, vol. 659, no. 1, pp. 106–135, Dec. 2011, ISSN: 0168-9002. DOI: 10.1016/j.nima.2011.06.067.

[20] M. A. Acero, P. Adamson, L. Aliaga, *et al.*, « First measurement of neutrino oscillation parameters using neutrinos and antineutrinos by NOvA », *Phys. Rev. Lett.*, vol. 123, p. 151 803, 15 Oct. 2019. DOI: 10.1103/PhysRevLett.123.151803.

[21] W. RODEJOHANN, « Neutrino-less double beta decay and particle physics », *International Journal of Modern Physics E*, vol. 20, no. 09, pp. 1833–1930, 2011. DOI: 10.1142/S0218301311020186.

[22] R. Castillo Fernandez, « T2K off-axis cross section measurements », *Proceedings of Science*, vol. NUFACT2014, p. 049, 2015. DOI: 10.22323/1.226.0049.

[23] K. Abe, H. Aihara, A. Ajmi, *et al.*, *T2K ND280 Upgrade – Technical Design Report*, 2020. arXiv: 1901.03750 [physics.ins-det].

[24] H.-K. Proto-Collaboration, : K. Abe, *et al.*, *Hyper-kamiokande design report*, 2018. arXiv: 1805.04163 [physics.ins-det].

[25] K. Abe, N. Akhlaq, R. Akutsu, *et al.*, « Improved constraints on neutrino mixing from the T2K experiment with 3.13×10^{21} protons on target », *Physical Review D*, vol. 103, no. 11, Jun. 2021, ISSN: 2470-0029. DOI: 10.1103/physrevd.103.112008.

[26] T. Dealtry, *Hyper-kamiokande*, 2019. arXiv: 1904.10206 [hep-ex].

[27] K. Hagiwara, N. Okamura, and K.-i. Senda, « The earth matter effects in neutrino oscillation experiments from Tokai to Kamioka and Korea », *Journal of High Energy Physics*, vol. 2011, no. 9, Sep. 2011, ISSN: 1029-8479. DOI: 10.1007/jhep09(2011)082.

[28] *Website of the NuFIT collaboration*. [Online]. Available: https://www.nu-fit.org.

[29] I. Esteban, M. Gonzalez-Garcia, M. Maltoni, T. Schwetz, and A. Zhou, « The fate of hints: updated global analysis of three-flavor neutrino oscillations », *Journal of High Energy Physics*, vol. 2020, no. 9, Sep. 2020, ISSN: 1029-8479. DOI: 10.1007/jhep09(2020)178.

[30] L. Kormos, Ed., *Proceedings of the 23rd International Workshop on Neutrino Factories, Superbeams and Beta Beams (NuFACT2022)*, University of Utah, Salt Lake City, Utah, USA, Jul. 2022.

[31] J. A. Formaggio and G. P. Zeller, « From ev to eev: neutrino cross sections across energy scales », *Reviews of Modern Physics*, vol. 84, no. 3, pp. 1307–1341, Sep. 2012, ISSN: 1539-0756. DOI: 10.1103/revmodphys.84.1307.

APPENDIX

1. NuFit

NuFIT 5.3 (2024)

		Normal Ordering (best fit)		Inverted Ordering ($\Delta\chi^2 = 2.3$)	
		bfp $\pm 1\sigma$	3σ range	bfp $\pm 1\sigma$	3σ range
without SK atmospheric data	$\sin^2\theta_{12}$	$0.307^{+0.012}_{-0.011}$	$0.275 \to 0.344$	$0.307^{+0.012}_{-0.011}$	$0.275 \to 0.344$
	$\theta_{12}/^\circ$	$33.66^{+0.73}_{-0.70}$	$31.60 \to 35.94$	$33.67^{+0.73}_{-0.71}$	$31.61 \to 35.94$
	$\sin^2\theta_{23}$	$0.572^{+0.018}_{-0.023}$	$0.407 \to 0.620$	$0.578^{+0.016}_{-0.021}$	$0.412 \to 0.623$
	$\theta_{23}/^\circ$	$49.1^{+1.0}_{-1.3}$	$39.6 \to 51.9$	$49.5^{+0.9}_{-1.2}$	$39.9 \to 52.1$
	$\sin^2\theta_{13}$	$0.02203^{+0.00056}_{-0.00058}$	$0.02029 \to 0.02391$	$0.02219^{+0.00059}_{-0.00057}$	$0.02047 \to 0.02396$
	$\theta_{13}/^\circ$	$8.54^{+0.11}_{-0.11}$	$8.19 \to 8.89$	$8.57^{+0.11}_{-0.11}$	$8.23 \to 8.90$
	$\delta_{\rm CP}/^\circ$	197^{+41}_{-25}	$108 \to 404$	286^{+27}_{-32}	$192 \to 360$
	$\frac{\Delta m^2_{21}}{10^{-5}\ \text{eV}^2}$	$7.41^{+0.21}_{-0.20}$	$6.81 \to 8.03$	$7.41^{+0.21}_{-0.20}$	$6.81 \to 8.03$
	$\frac{\Delta m^2_{3\ell}}{10^{-3}\ \text{eV}^2}$	$+2.511^{+0.027}_{-0.027}$	$+2.428 \to +2.597$	$-2.498^{+0.032}_{-0.024}$	$-2.581 \to -2.409$
		Normal Ordering (best fit)		Inverted Ordering ($\Delta\chi^2 = 9.1$)	
		bfp $\pm 1\sigma$	3σ range	bfp $\pm 1\sigma$	3σ range
with SK atmospheric data	$\sin^2\theta_{12}$	$0.307^{+0.012}_{-0.011}$	$0.275 \to 0.344$	$0.307^{+0.012}_{-0.011}$	$0.275 \to 0.344$
	$\theta_{12}/^\circ$	$33.67^{+0.73}_{-0.71}$	$31.61 \to 35.94$	$33.67^{+0.73}_{-0.71}$	$31.61 \to 35.94$
	$\sin^2\theta_{23}$	$0.454^{+0.019}_{-0.016}$	$0.411 \to 0.606$	$0.568^{+0.016}_{-0.021}$	$0.412 \to 0.611$
	$\theta_{23}/^\circ$	$42.3^{+1.1}_{-0.9}$	$39.9 \to 51.1$	$48.9^{+0.9}_{-1.2}$	$39.9 \to 51.4$
	$\sin^2\theta_{13}$	$0.02224^{+0.00056}_{-0.00057}$	$0.02047 \to 0.02397$	$0.02222^{+0.00069}_{-0.00057}$	$0.02049 \to 0.02420$
	$\theta_{13}/^\circ$	$8.58^{+0.11}_{-0.11}$	$8.23 \to 8.91$	$8.57^{+0.13}_{-0.11}$	$8.23 \to 8.95$
	$\delta_{\rm CP}/^\circ$	232^{+39}_{-25}	$139 \to 350$	273^{+24}_{-26}	$195 \to 342$
	$\frac{\Delta m^2_{21}}{10^{-5}\ \text{eV}^2}$	$7.41^{+0.21}_{-0.20}$	$6.81 \to 8.03$	$7.41^{+0.21}_{-0.20}$	$6.81 \to 8.03$
	$\frac{\Delta m^2_{3\ell}}{10^{-3}\ \text{eV}^2}$	$+2.505^{+0.024}_{-0.026}$	$+2.426 \to +2.586$	$-2.487^{+0.027}_{-0.024}$	$-2.566 \to -2.407$

Figure 11 *– Three-flavor oscillation parameters from the NuFIT fit to global data as of March 2024. The results shown in the upper (lower) section are obtained without (with) the inclusion of the tabulated χ^2 data on atmospheric neutrinos provided by the Super-Kamiokande collaboration (SK-atm). Extracted from [28]. See also [29].*

2. Exact oscillation probability in matter

The exact oscillation probability for a muon (anti-)neutrino to oscillate into an electron (anti-)neutrino, at an energy E and after a distance L is given [30] by

$$\begin{aligned}\mathcal{P}_{\mu\to e}(E,L) = {} & 4\,{c_{13}}^2{s_{13}}^2\sin^2(X_{31})\left(1 \pm \frac{2A}{\Delta m^2_{31}}\left(1-{s_{13}}^2\right)\right) \\ & + 8\,{c_{13}}^2 s_{12}s_{13}s_{23}\left(c_{12}c_{23}\cos(\delta_{\rm CP}) - s_{12}s_{13}s_{23}\right)\cos(X_{32})\sin(X_{31})\sin(X_{21}) \\ & \mp 8\,{c_{13}}^2{s_{13}}^2{s_{23}}^2\cos(X_{32})\sin(X_{31})\frac{AL}{4E}\left(1-2{s_{13}}^2\right) \\ & \mp 8\,{c_{13}}^2 c_{12}c_{23}s_{12}s_{13}s_{23}\sin(\delta_{\rm CP})\sin(X_{32})\sin(X_{31})\sin(X_{21}) \\ & + 4\,{s_{12}}^2{c_{13}}^2\left(c_{12}c_{23} + {s_{12}}^2{s_{13}}^2{s_{23}}^2 - 2\,c_{12}c_{23}s_{12}s_{13}s_{23}\cos(\delta_{\rm CP})\right)\sin^2(X_{21})\end{aligned} \tag{21}$$

where we used the notation previously defined, and where we denote $A \equiv 2\sqrt{2}G_F n_e E$ coming from the matter effects, and where the + (resp. −) sign raises for neutrinos (resp. antineutrinos). In this formula, the first term on the right-hand side is the leading term, the second is CP conserving, the third is due to matter effects, the fourth is CP violating and the last one is the solar term.

3. Neutrino CC cross-sections

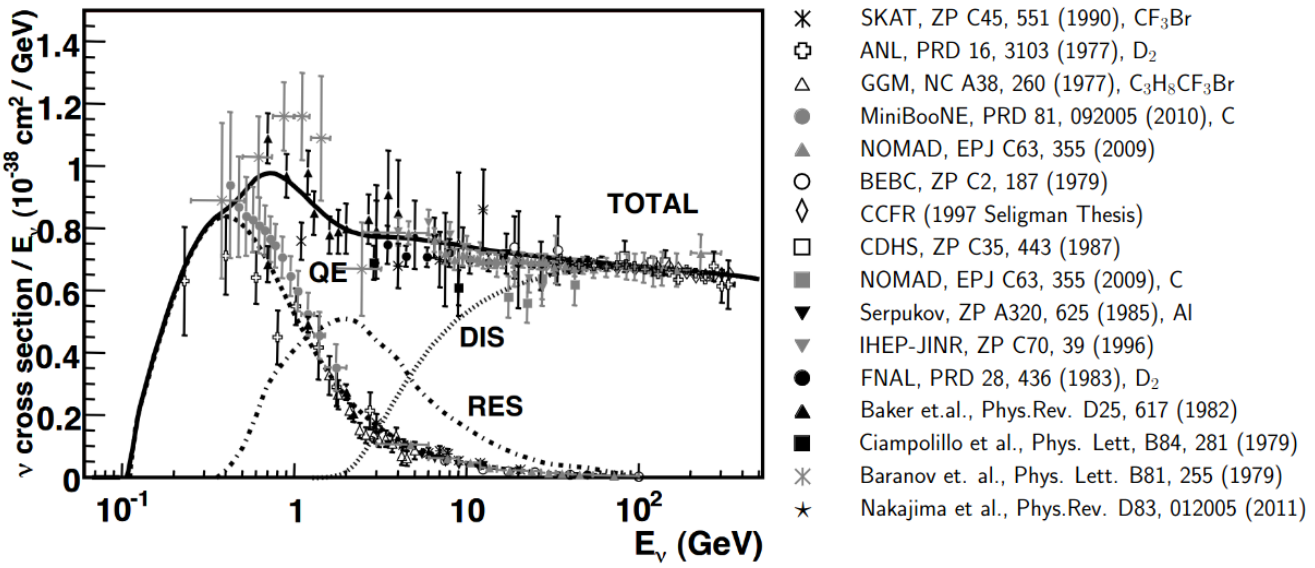

Figure 12 *– Total neutrino and antineutrino per nucleon CC cross sections (for an isoscalar target) divided by neutrino energy and plotted as a function of energy. These contributions include quasi-elastic scattering (dashed), resonance production (dot-dash), and deep inelastic scattering (dotted). Extracted from [31].*